

# Precipitation hardening in an Al-Cu-Si-Mg alloy at 130 to 220°C

W. BONFIELD

*Department of Materials, Queen Mary College, London, UK*

P. K. DATTA

*Department of Chemistry and Metallurgy, Glasgow College of Technology, Glasgow, UK*

The variation of the hardness of a complex Al alloy, of the L70 type, (Al 4% Cu 0.8% Si 0.8% Mg 0.7% Mn 0.5% Fe) with ageing time at 130, 160 and 190°C was measured and correlated with transmission electron microscope observations of precipitate morphology. It was established that the peak hardness, after both 160 and 190°C ageing, was associated with coherent  $\theta'$  precipitate particles with a diameter of  $\sim 700 \text{ \AA}$  and the subsequent limited overageing at these temperatures was controlled by the slow growth of  $\theta'$  particles. Measurements of  $\theta'$  particle coarsening at 220°C suggested that the process occurred by Ostwald ripening. In contrast, ageing at 130°C gave a series of hardness-time plateaus, which were ascribed to the sequential precipitation of zones,  $\theta''$  and  $\theta'$  precipitates.

## 1. Introduction

Although the complex aluminium precipitation hardening alloy, of L70 type, and with composition Al 4% Cu 0.8% Si 0.8% Mg 0.7% Mn 0.5% Fe\*, finds considerable application, the precipitate morphology associated with peak hardness in this alloy has not previously been established. In this paper the ageing behaviour at 130, 160, 190 and 220°C is discussed. The variation of hardness with ageing time was measured and is correlated with transmission electron microscope observations of precipitate morphology.

## 2. Experimental procedure

The Al alloy, of composition shown in Table I, in sheet form (thickness = 1.25 mm), was solution treated at 500°C for 2 h, and quenched in water at

room temperature. The quenched specimens were then aged at 130, 160 and 190°C for various times up to 1000 h and the corresponding hardness values (VHN), (the average of ten readings and accurate to  $\pm 5$  VHN), were determined. Thin foils were prepared from the aged specimens (and from some specimens aged at 220°C) and examined in a JEOL-JEM7 electron microscope.

## 3. Results

### 3.1. Hardness measurements

The hardness-ageing time graphs measured at 130, 160 and 190°C are shown in Fig. 1. At 130°C, the hardness-ageing time graph exhibited four hardness plateaus, at 128 VHN (after 15 h), at 135 VHN (after 40 h), at 150 VHN (after 80 h) and at the peak hardness of 162 VHN. In contrast, at 160°C peak hardness (163 VHN) was achieved after 20 h and remained constant until 50 h. A pronounced reduction in hardness occurred after 200 h and a value of 135 VHN was measured after 1000 h. The ageing curve at 190°C was similar in form to that at 160°C, but the time to reach peak hardness (160 VHN) was only 13 h and pro-

TABLE I Composition of Al alloy

Element	wt %	Element	wt %
Cu	4	Fe	0.5
Si	0.8	Ni	0.004
Mg	0.8	Al	rest
Mn	0.7		

\* Wt. %

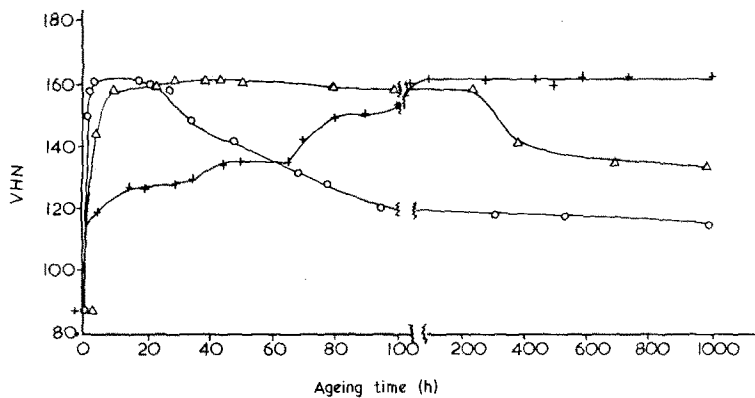


Figure 1 Hardness (VHN) versus ageing time at 130°C (+), 160°C (Δ) and 190°C (○). (Note change in scale at 100 h.)

nounced softening started after 18 h, with a value of 115 VHN after 100 h.

### 3.2. Precipitate morphology

#### 3.2.1. Ageing at 130°C

The as-quenched specimens exhibited helical dislocations, numerous insoluble particles [1] and a mottled background structure, such as shown in Fig. 2. This structure persisted until an ageing time

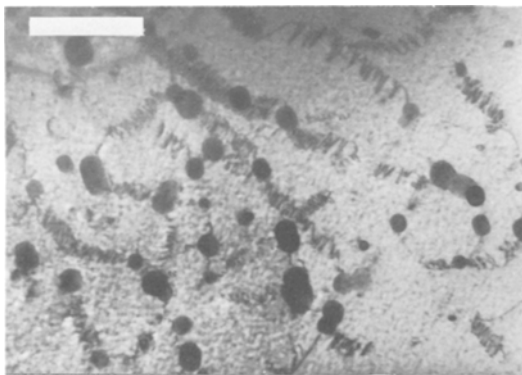


Figure 2 Helical dislocations, insoluble particles and mottled background in an as-quenched specimen (1 μm marker).

of 80 h at 130°C, when  $\theta''$  precipitate particles, with extensive strain fields, were also resolved (Fig. 3a) and faint (100) matrix spot streaking was noted in the selected area diffraction patterns (Fig. 3b). The precipitate particles without extensive strain fields, which can also be seen in Fig. 3a, were probably  $\theta'$  precipitate particles, but  $\theta'$  precipitate diffraction spots were not definitely until after 150 h at 130°C, as shown in Fig. 4. The associated streaking of  $\theta'$  diffraction spots in Fig. 4 indicates the presence of coherency strain, which was retained for all the ageing times examined (up to 504 h).

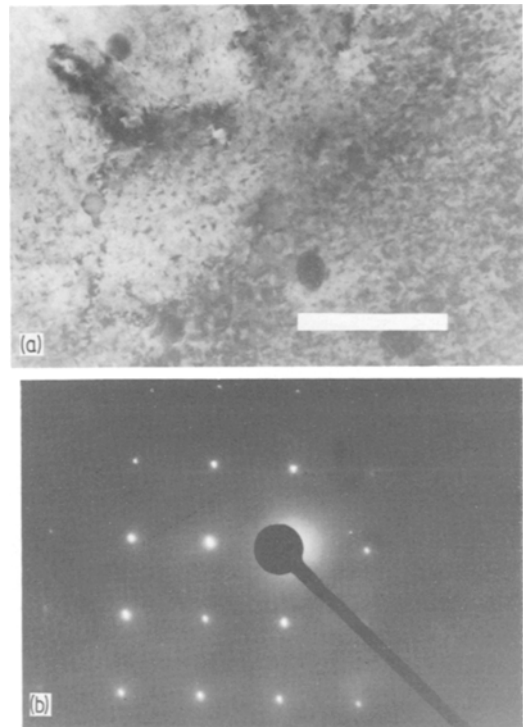


Figure 3(a)  $\theta''$  and  $\theta'$  precipitate particles (and some insoluble particles) after 80 h at 130°C (1 μm marker). (b). Diffraction pattern from (a) showing faint (100) matrix spot streaking.

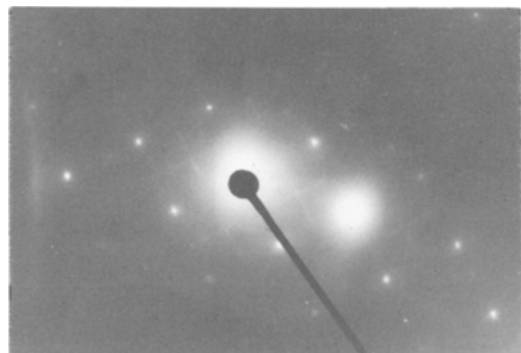


Figure 4  $\theta'$  precipitate diffraction spots showing pronounced streaking, after 150 h at 130°C.

No evidence of  $S'$  or  $S$  precipitate ( $Al_2CuMg$ ) was noted at any of the ageing temperatures investigated.

### 3.2.2. Ageing at 160 and 190°C

The initial ageing sequence at 160 and 190°C occurred more rapidly than at 130°C. At both temperatures, the onset of  $\langle 100 \rangle$  matrix spot streaking (after 1 h) was observed before  $\theta''$  precipitate was resolved (after 2 h, as in Fig. 3a) while the presence of  $\theta'$  precipitate diffraction spots (with associated streaking) was noted after 3 h (Fig. 5b).

Further ageing increased the diameter of the  $\theta'$  precipitate (Figs. 6, 7), although the rate of increase was small, and increased, and finally

decreased, the number of  $\theta'$  precipitate particles per unit volume (Fig. 8). In these figures, the precipitate diameter ( $d$ ) refers to the dimension of the precipitate measured from a  $\{001\}$  foil surface, while the number of particles per unit volume  $N_v$  was calculated from:

$$N_v = \frac{N_A}{t + d} \quad (1)$$

where  $N_A$  is number of particles per unit area of a  $\{001\}$  foil surface and  $t$  is the foil thickness ( $\sim 3000 \text{ \AA}$ ). The number of  $\theta'$  particles per unit volume was a maximum after  $\sim 200 \text{ h}$  at 160°C and  $\sim 80 \text{ h}$  at 190°C, while the diameter of  $\theta'$  increased from  $\sim 700 \text{ \AA}$  (3 to 45 h) to  $\sim 950 \text{ \AA}$  (640 h) at 160°C, as compared with an increase

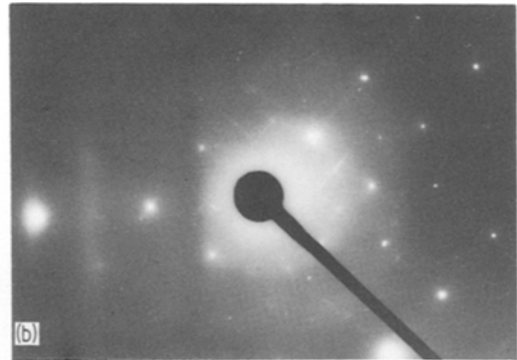
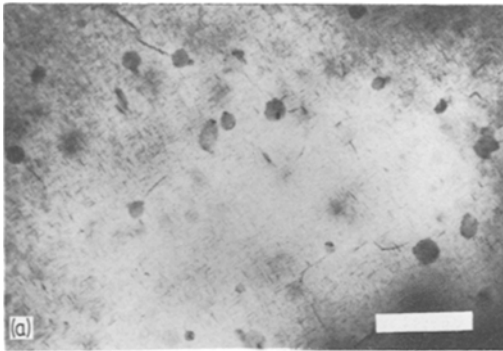


Figure 5(a)  $\theta'$  precipitate particles, after 3 h at 190°C (1  $\mu\text{m}$  marker). (b) Diffraction pattern from (a), showing pronounced  $\theta'$  diffraction spot streaking.

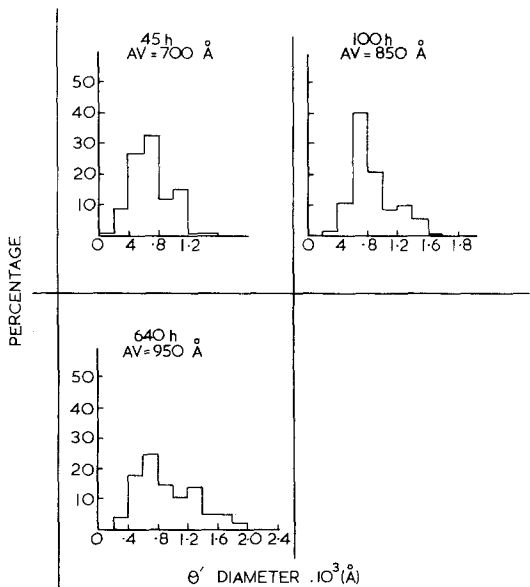


Figure 6 Histograms of  $\theta'$  particle diameter, after various ageing times at 160°C.

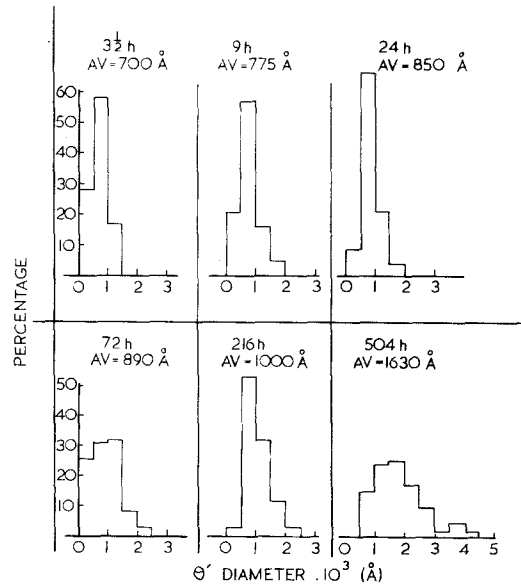


Figure 7 Histograms of  $\theta'$  particle diameter after various ageing times at 190°C.

Figure 8 The variation of the number of  $\theta'$  particles per unit volume with ageing time at 160°C ( $\Delta$ ) and 190°C ( $\circ$ ).

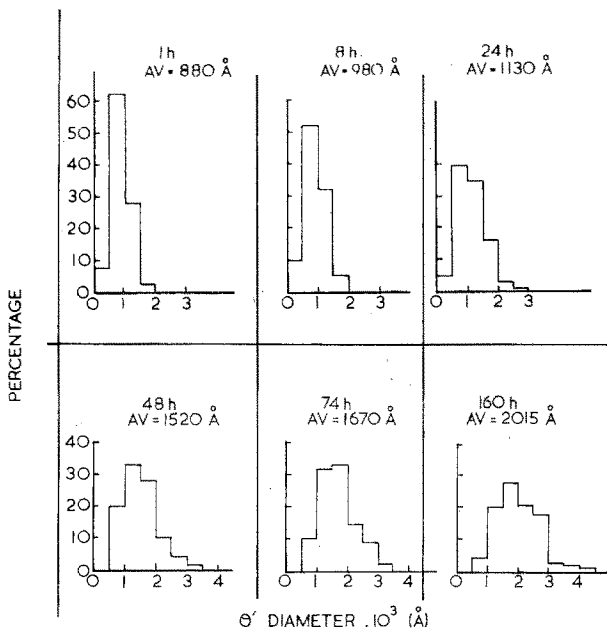
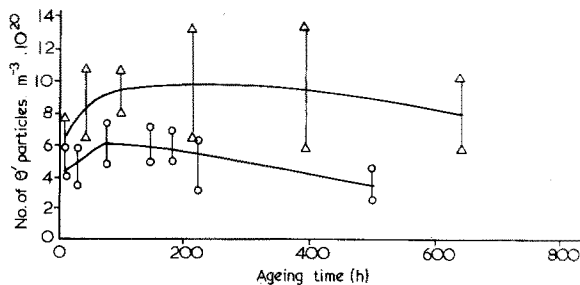
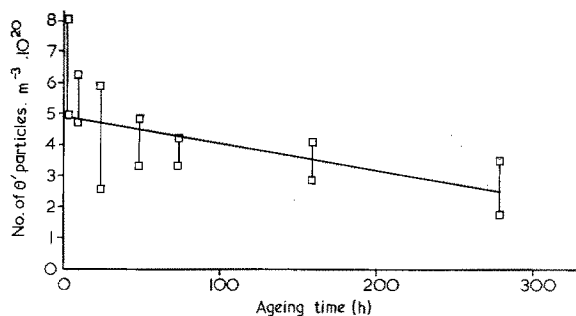


Figure 9 Histograms of  $\theta'$  particle diameter after various ageing times at 220°C.

Figure 10 The variation of the number of  $\theta'$  particles per unit volume with ageing time at 220°C ( $\square$ ).



from  $\sim 700 \text{ \AA}$  ( $3\frac{1}{2} \text{ h}$ ) to  $\sim 1630 \text{ \AA}$  (504 h) at 190°C. Some streaking through  $\theta'$  diffraction spots was associated with all these conditions, except for the 504 h at 190°C ageing treatment.

### 3.2.3. Ageing at 220°C

For ageing times at 160 and 190°C at which the increase in  $\theta'$  precipitate diameter is accompanied by a decrease in the number of  $\theta'$  particles per unit volume, it would be expected that particle coarsening occurs by the resolution of smaller particles and the growth of larger particles (Ostwald

ripening). However, as the data in this region at 160 and 190°C were limited, the increase of  $\theta'$  particle diameter with time was also investigated at higher ageing temperature. At 220°C, the  $\theta'$  precipitate diameter increased from 880 Å (after 1 h) to 2015 Å (after 160 h), as shown in Fig. 9, while the number of  $\theta'$  particles per unit volume continuously decreased (Fig. 10). Even at this temperature  $\theta'$  diffraction spot streaking was observed after 240 h.

## 4. Discussion

It has been established that the peak hardness

produced by ageing at 160 and 190°C has approximately the same value and in each case is correlated with the presence of  $\theta'$  precipitate.

At both temperatures, the peak hardness–time plateau is associated with an average  $\theta'$  diameter of  $\sim 700$  Å and a continuing increase in the number of  $\theta'$  particles per unit volume (although with different absolute values at each temperature). At 160°C, the onset of a marked decrease in hardness with time (at 200h) relates to an average  $\theta'$  diameter of 850 to 950 Å and corresponds with the maximum number of particles per unit volume. A similar value of  $\theta'$  diameter (850 Å) is associated with the onset of overageing at 190°C, although the number of particles per unit volume is less than the maximum value. The limited progress of overageing at both 160 and 190°C results from the measured slow growth rate of the  $\theta'$  particles and the consequent retention of coherency strain. The effects of  $\theta'$  particle diameter on hardness at 160 and 190°C are similar during overageing, with, for example, a hardness of 133 VPN corresponding to 640h at 160°C ( $\theta' \sim 950$  Å) and 72h at 190°C ( $\theta' \sim 890$  Å).

The rate of  $\theta'$  particle coarsening at 220°C can be evaluated in terms of the equation derived [2] for Ostwald ripening of spheroidal particles, with, for a given temperature and composition,

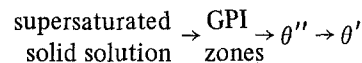
$$r^3 - r_0^3 = k(t - t_0) \quad (2)$$

where  $r$  and  $r_0$  are the mean  $\theta'$  particle radii at time  $t$  and  $t_0$  (the onset of coarsening) and  $k$  is a constant. As  $\theta'$  particles are disc-shaped rather than spheroidal, it is assumed in using Equation 2 that the thickness increased at the same rate as the radius. Taking  $t_0 = 1$  h, a plot of  $(r^3 - r_0^3)$  versus  $(t - t_0)$  exhibits a linear relationship (Fig. 11) and confirms that at 220°C coarsening of  $\theta'$  occurs by

the resolution of the smaller particles and growth of the larger particles. For comparison, the two data points at 190°C, calculated on the basis that  $t_0 = 72$  h are also plotted in Fig. 11.

In contrast to ageing at 160 and 190°C, the peak hardness after ageing at 130°C was associated with a structure consisting of  $\theta'$  precipitate and  $\theta''$  precipitate, which produced an equivalent value.

At 160 and 190°C, the appearance of  $\langle 100 \rangle$  matrix spot streaking (after 1 h), before that of  $\theta''$  precipitate (after 2 h), may be correlated with the presence of GPI zones. Hence the likely major ageing sequence appears as:



However, this sequence does not account for the increase during the first hour of ageing at 160 and 190°C, while the first 80 h of ageing at 130°C produced a considerable increase in hardness without any  $\langle 100 \rangle$  matrix spot streaking. This increase in hardness at 130°C may be related to the presence of GPB zones (Al–Cu–Mg) [3] which produce smaller lattice strains than GPI zones, and have been noted [4, 5] in both Al 2.5% Cu 1.2% Mg and Al 2.5% Cu 1.2% Mg 0.24% Si. GPI and GPB zones have been observed together in a Cu–Mg alloy [3] with a Cu:Mg ratio of 7:1, but in each case the zones were succeeded by  $\theta''$  and  $\theta'$  precipitate or  $S'$  and  $S$  (Al<sub>2</sub>CuMg) precipitate, respectively. In the present study, no  $S'$  precipitate was observed, which on the basis of this previous evidence, suggests that the GPB zones persist throughout the ageing sequence, with  $\theta'$  precipitate developing from either the limited number of GPI zones or by direct nucleation. This point is considered in detail elsewhere in the context of

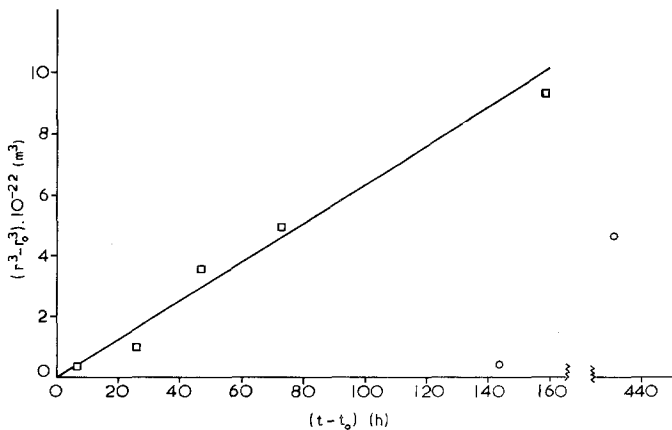


Figure 11 Coarsening of  $\theta'$  particles at 220°C (□) and 190°C (○).

quenching and room temperature ageing of this alloy [6]. The variations in slope of the time curve observed during the approach to peak hardness at 130° C probably reflect the sequential precipitation of zone(s) to  $\theta''$  to  $\theta'$ , while the rapidity of initial ageing at 160 and 190° C precludes any distinction between these intermediate phases.

## 5. Conclusions

(1) The peak hardness produced by 160 and 190° C ageing is related to coherent  $\theta'$  precipitate particles of  $\sim 700$  Å diameter, while at 130° C, peak hardness is associated with a mixed structure of  $\theta'$  and  $\theta''$  precipitate.

(2) The rate of  $\theta'$  particle coarsening is slow at 160 and 190° C and, at 220° C is associated with Ostwald ripening.

## Acknowledgements

The provision of an equipment and maintenance

grant (PKD) for this research by the Ministry of Defence (Procurement Executive) is gratefully acknowledged, together with the continuing support of Mr C. R. Milne and Mr M. Trapaud of the Avionics (now Radio and Navigation) Division, Royal Aircraft Establishment and useful discussions with Dr R. N. Wilson of the Materials Department, Royal Aircraft Establishment.

## References

1. P. K. DATTA, Ph. D. Thesis, University of London (1974).
2. C. WAGNER, *Z. Electrochem.* **65** (61) 581.
3. J. M. SILCOCK, *J. Inst. Metals* **89** (1960) 203.
4. R. N. WILSON *ibid* **97** (1969) 80.
5. R. N. WILSON, D. M. MOORE and P. J. E. FORSYTH, *ibid* **95** (1967) 177.
6. W. BONFIELD and P. K. DATTA, to be published.

Received 12 January and accepted 13 February 1976.